Torque comparison of surface mount and interior permanent magnet synchronous motor for railway applications

Polater, Nursaid; Kamel, Tamer; Tricoli, Pietro

DOI:
10.1109/CPE-POWERENG50821.2021.9501196

Document Version
Peer reviewed version

Citation for published version (Harvard):
Polater, N, Kamel, T & Tricoli, P 2021, Torque comparison of surface mount and interior permanent magnet synchronous motor for railway applications. in *2021 IEEE 15th International Conference on Compatibility, Power Electronics and Power Engineering (CPE-POWERENG)*., 9501196, Compatibility in Power Electronics (CPE), Institute of Electrical and Electronics Engineers (IEEE), pp. 1-6, IEEE CPE-POWERENG 2021, Florence, Italy, 14/07/21. https://doi.org/10.1109/CPE-POWERENG50821.2021.9501196

Torque Comparison of Surface Mount and Interior Permanent Magnet Synchronous Motor for Railway Applications

Nursaid Polater
Department of Electronic, Electrical and Computer Engineering
University of Birmingham
Birmingham, UK
nxp857@student.bham.ac.uk

Tamer Kamel
Department of Electronic, Electrical and Computer Engineering
University of Birmingham
Birmingham, UK
t.kamel@bham.ac.uk

Pietro Tricoli
Department of Electronic, Electrical and Computer Engineering
University of Birmingham
Birmingham, UK
p.tricoli@bham.ac.uk

***Abstract*— This research study investigates the design of field-oriented control (FOC) for permanent magnet synchronous machines (PMSM), used for railway applications. The study aims to examine the speed and the torque control methods as well as the torque contribution of the saliency by implementing the field weakening (FW) and the maximum torque per amp (MTPA) techniques. The FW strategy provides a wider speed spectrum for the motors, and on the other hand, the MTPA enables higher output torque with better efficiency, as illustrated in the preliminary findings. Therefore, these strategies appear suitable for controlling the PMSM in electrified transport applications as validated in this study through the MATLAB/Simulink platform.**

Keywords*— *Field weakening, Field oriented control, Maximum torque per ampere, Permanent magnet synchronous motors

I. INTRODUCTION

Railway transport systems have existed since the 18th century and are currently growing [1]. With reference to the traction systems, induction machine (IM) took over from DC motors when power converters with forced commutation became commercially available [2, 3].

Railway traction motors have typically a requirement of high-power density and efficiency. Therefore, the highest power density of permanent magnet synchronous motors (PMSMs) compared to induction motors is seen as clear advantage for traction application [4, 5]. On the other hand, one of the main drawbacks is the need of dedicated inverter for each motor, that has an impact on cost and reliability [6, 7]. A light railway typically has 6 to 8 traction motors and less inverters are employed if induction motors are used. For the PMSM, individual inverters are needed to eleminate torque ripples because of synchronous reactance and moment of inertia [8]. Once two PMSMs shared a common inverter, controlling of the current will be difficult due to the position of poles are different from each other. For this reason, the generated torque will consist vibration in multi motor traction system.

This research study investigates the design of the field-oriented control (FOC) for three-phase PMSMs for railway applications. As a result, the study analyses the implementation of field weakening (FW) and maximum torque per amp (MTPA) methods. Main contribution of this article is providing a comparison of torque level of surface type and interior PMSM as well as understanding controllability and complexity of FW/MTPA strategies for high power PMSMs employed in railway applications.

The paper starts with a brief description of the PMSM in section II along with its input/output characteristics. After that, the FW and MTPA algorithms are introduced in sections III and IV, respectively. Finally, section V shows the simulation results obtained with a simulation model in MATLAB/Simulink.

II. PERMANENT MAGNET SYNCHRONOUS MOTOR

PMSMs are getting popular amongst the other motors for transportation applications and gaining attention for railway traction. PMSM machines can be classified as brushless AC and DC machines. Both are synchronous machines, but back-EMF is sinusoidal in AC machines, and trapezoidal DC machines, respectively. Additionally, current excitation waveforms are different as well. Whereas the brushless AC machine has sinusoidal current excitation, the brushless DC machine has square wave excitation. Moreover, PMSMs are classified as a surface mount (SM), inset and interior permanent magnet (IPM) machine in terms of magnet locations within the rotor [9].

There are a couple of PMSM manufacturers for railway applications. For instance, Toshiba has launched traction motors for 1000/1600 series Tokyo commuter trains with a power of approximately 200 kW. In addition, Toshiba produced an 80 kW PMSM for a diesel hybrid shunting locomotive. Siemens and Alstom offer innovative permanent-magnet synchronous motors, including gearless direct drives as well.

In PMSM, when an alignment torque is produced by the interaction between the magnets and the stator magnetic field. Interior and inset machines, have magnetic saliency, so the stator flux linkage is variable because reluctance changes while the rotor rotates. This flux linkage produces a reluctance torque that, depending on the saliency and the current, can increase the electromagnetic torque.

For railway applications, there are two operating regions of the motor, which are current and voltage limiting regions, also known as constant torque region, and the constant power region where torque is approximately decreased inversely proportional to speed up to the maximum speed of the train.

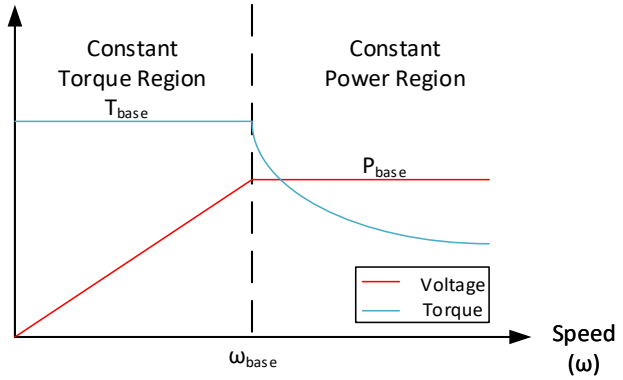

Fig. 1 Speed Range (CVCP) *[10]*

In order to get good motor performance for the whole speed range, the other one is the maximum torque per amp (MTPA) strategy can be used for the constant torque region, while field weakening (FW) can be used for the constant power region.

The MTPA strategy is different for SMPMSM and IPMSM. In SMPMSM, the direct current component, i_d, is typically set to zero, as it does not contribute to the torque, but it contributes to the machine copper losses. Conversely, i_d contributes to the reluctance torque of IPMSM, therefore the value achieving lowest losses depends on the mechanical speed.

FW enables the extension of speed range beyond the base speed, albeit with a lower maximum torque [11]. For traction applications, the maximum speed is typically between 2 and 3 times the base speed. In PMSMs, the flux linkage is weakened by injecting a negative current i_d above the base speed, which means that the maximum current quadrature i_q must be reduced to ensure that the current rating of the motor is not exceeded [8].

The mathematical model of PMSMs is given by the following voltage equations, written in the rotating reference frame (RF) synchronous with the rotor:

$$\begin{aligned} v_d &= R_s i_d + \frac{d\psi_d}{dt} - \omega_e \psi_q \\ v_q &= R_s i_q + \frac{d\psi_q}{dt} + \omega_e \psi_d \end{aligned} \tag{1}$$

Where v_d and v_q are the direct and quadrature stator voltages, Rs is the stator winding resistance, ω_e is the electrical angular speed of a machine, and ψ_d and ψ_q are the direct and quadrature components of the flux linkage, equal to:

$$\begin{aligned} \psi_d &= L_d i_d + \psi_m \\ \psi_q &= L_q i_q \end{aligned} \tag{2}$$

Where L_d and L_q are the direct and quadrature inductance, and ψ_m is the permanent magnet flux linkage.

Finally, the torque equation is:

$$T = \frac{3}{2} p[\psi_m i_q + \frac{1}{2}(L_d - L_q) i_d i_q] \tag{3}$$

Where p is the number of pole pairs.

III. MTPA Strategy

The MPTA strategy provides desired torque level with minimum current for the stator windings. As mentioned before, it minimises copper losses and maximises the overall efficiency of the motor [12]. From (3), the locus of the torque as a function of i_d and i_q is an ellipse. As shown in Fig, 2, there is an optimal value of the current magnitude.

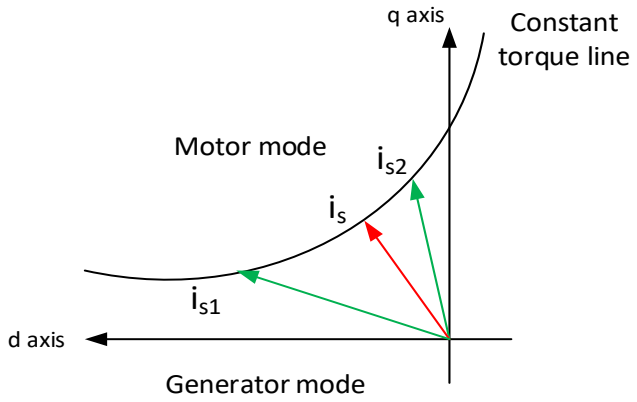

Fig. 2 Vector representation of the minimum stator current vector at a given torque level for an IPMSM *[13]*

Therefore, the MTPA curve is given by the locus of the optimal current for each value of the torque [12]. Expressing the d and q components of the current as a function of the current magnitude, i, and angle,γ, (3) can be rewritten as:

$$T = \frac{3}{2} p[\psi_m i \sin\gamma + \frac{i^2}{2} \sin 2\gamma \, (L_d - L_q)] \tag{4}$$

$$\begin{aligned} i_d &= -i \sin\gamma \\ i_q &= i \cos\gamma \end{aligned} \tag{5}$$

As shown in Fig. 3, the torque angle corresponding to the maximum reluctance torque is different from the maximum developed electromagnetic torque.

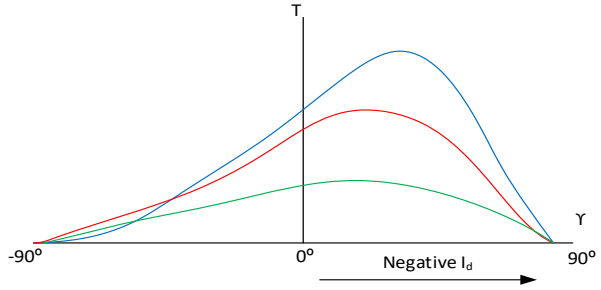

Fig. 3 Curves of reluctance (green), magnetic (red) and total developed torque (blue) *[9]*

The maximum torque is given by the derivative of (4)

$$\frac{dT}{d\gamma} = \frac{3}{2} p[\psi_m i \cos\gamma - i^2 \cos 2\gamma \, (L_d - L_q)] \tag{6}$$

As in PMSM motor for traction is usually, L_q greater than L_d that means there is positive reluctance torque and, the optimal torque angle is larger than 90°. As a result, d and q axes' currents are expressed as:

$$i_{dm} = \frac{\psi_m - \sqrt{{\psi_m}^2 + 8(L_q - L_d)^2 i^2}}{4(L_q - L_d)} \tag{7}$$

$$i_{qm} = \sqrt{i^2 - {i_{dm}}^2}$$

IV. Field Weakening

As well-known, to increase the speed it is necessary to reduce the flux linkage to limit the motor voltage to the rated value, as the back EMF is directly proportional to the speed.

The analysis of FW operations can be simplified if the stator resistance is assumed equal to zero and steady-state operations are considered in (1), which yields:

$$\begin{aligned} v_d &= -\omega_e L_q i_q \\ v_q &= \omega_e L_d i_d + \omega_e \psi_m \end{aligned} \tag{8}$$

From (8) the stator terminal voltage in $V_s = \sqrt{v_d^2 + v_q^2}$, and electrical speed are respectively:

$$\begin{aligned} V_s &= \sqrt{(\omega_e L_q i_q)^2 + (\omega_e L_d i_d + \omega_e \psi_m)^2} \\ \omega_e &= \frac{V_s}{\sqrt{(L_d i_d + \psi_m)^2 + (L_q i_q)^2}} \end{aligned} \tag{9}$$

There are a few field-weakening control strategies for both SMPMSM and IPMSM motors. In this paper, constant voltage constant power (CVCP) control will be employed for SMPMSM, voltage and current limited maximum torque (VCLMT) control for IPMSM [14].

CVCP control is the most suitable algorithm for SMPMSM owing to simple implementation and it requires fewer hardware components. In this method, output power is equal to rated power after base speed and is constant, as shown in Fig. 1. The equation of CVCP can be written as:

$$P_{base} = \frac{\omega_{base}}{p} T_{base} \tag{10}$$

As $i_d = 0$ up to the base speed for SMPMSM motors, i_q is equal to the rated current, therefore T_{base} can be written as:

$$T_{base} = \frac{3}{2} p \psi_m I_s \tag{11}$$

Substituting (10) into (9) yields:

$$\omega_e i_q = \omega_{base} I_s \tag{12}$$

Voltage equation is rewritten by substituting (12) into (8) as:

$$\begin{aligned} v_d &= -\omega_e L_q i_q = -L_q(\omega_{base} I_s) = constant \\ v_q &= \omega_{base} \psi_m = constant \end{aligned} \tag{13}$$

From the second of (12) we finally obtain:

$$\omega_e(\psi_m + L_d i_d) = \omega_{base} \psi_m \tag{14}$$

i_d and i_q are derived from (12) and (14).

$$\begin{aligned} i_d &= \frac{\omega_{base}}{\omega_e}\frac{\psi_m}{L_d} - \frac{\psi_m}{L_d} \\ i_q &= \frac{\omega_{base}}{\omega_e} I_s \end{aligned} \tag{15}$$

Although VCLMT control can be used in both SMPMSM and IPMSM, it has slightly different approach for IPMSM. For IPMSM, there are two constraints in FW operations, one being the current limit and the other being limit. Fig. 4 shows these limits that are respectively represented by a circle and an ellipse.

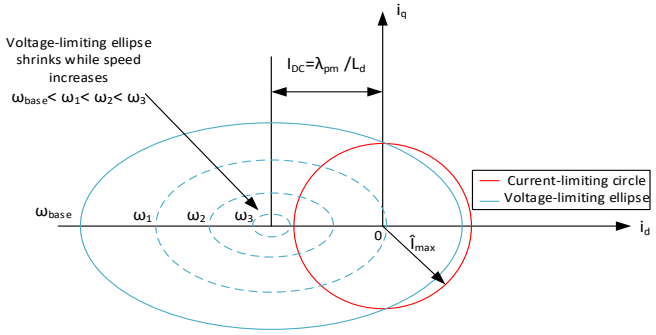

Fig. 4 Current-limiting circle and voltage-limiting ellipse for IPM motors *[15]*

$$\frac{[(\psi_m/L_d) + (i_d)]^2}{V_s^2/(\omega_e L_d)^2} + \frac{(i_q)^2}{V_s^2/(\omega_e L_q)^2} = 1 \tag{16}$$

The solutions for a given voltage and current are given by the intersection between the 2 curves that are given by:

$$\begin{aligned} i_{d1} &= \frac{-\psi_m L_d + \sqrt{(\psi_m L_d)^2 - (L_d^2 - L_q^2)[\psi_m^2 + L_q^2 I_{max}^2 - \left(\frac{V_{max}}{\omega_e}\right)^2]}}{(L_d^2 - L_q^2)} < 0 \\ i_{d2} &= \frac{-\psi_m L_d - \sqrt{(\psi_m L_d)^2 - (L_d^2 - L_q^2)[\psi_m^2 + L_q^2 I_{max}^2 - \left(\frac{V_{max}}{\omega_e}\right)^2]}}{(L_d^2 - L_q^2)} > 0 \end{aligned} \tag{17}$$

The negative i_d should be selected for FW operations, so the current is demagnetising.

V. Simulation Results

In this section, a simulation study of SMPMSM and IPMSM presented to show the main differences when used for railway traction. Table I shows the common parameters of the 2 machines.

Table I Datasheet of PMSM

Rated speed of motor (rpm)	1500
Base frequency (Hz)	50
Rated power (kW)	110
Rated voltage (V)	359
Rated current (A)	270
Stator phase resistance (Ω)	0.0088
Motor + Load Moment of Inertia ($kg.m^2$)	50.85
Magnetising inductance (mH)	0.897
Leakage inductance (mH)	0.207
Train maximum speed (km/h)	80
Train mass (tone)	18
Gear ratio	6
Wheel diameter (m)	0.6

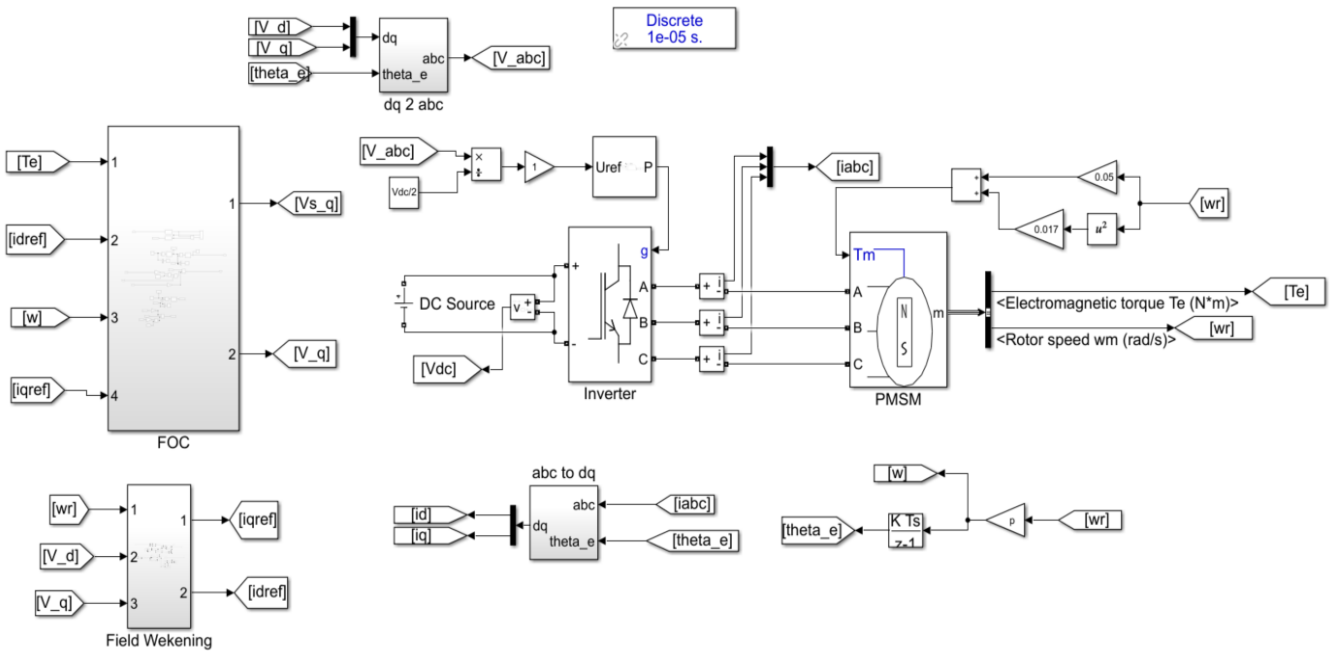

Fig. 5 Simulink Model of SMPMSM with FW

For the 2 machines, permanent magnet flux linkage is derived from first equation of (9) by assuming i_d=0 which is common control method for both machine up to base speed. Then (18) is used to get the permanent magnet flux linkages for the machines.

$$\psi_m = \frac{\sqrt{{V_s}^2 - (\omega_e L_q i_q)^2}}{\omega_e} \qquad (18)$$

After implementation of (18), permanent magnet flux linkage is 0.8335 for IPMSM and 0.8841 for SMPMSM. Some assumptions are made and equivalent moment of inertia of the railcar is needed to derive for the load of inertia. Therefore, typical weight of light railway parameters [16], gear ratio and wheel diameter [17], and equivalent moment [18, 19]are obtained separately.

Speed and current of the motor need PI regulator to operate within the machine limits and this PI regulators have parameters that requires to be tuned. Existence of variety tuning methods will make easier for determining of proportional and integral gains. All artificial intelligence techniques like fuzzy logic and traditional methods such as Ziegler-Nichols, pole placement etc. can be employed in order to tune the parameters. Amongst the given methods the pole placement is explained in [20] and utilised for tuning of K_p and K_I gains for both machines.

A model of SMPMSM was developed in Simulink as shown in Fig. 5. The L_d and L_q inductances of the model are sum of magnetising and leakage inductances and equal to 1.104 mH for both. The FW is implemented with a dynamic saturation block to control the voltage above the base speed. The limits of i_d and i_q references are derived according to the field weakening equations given in section IV.

Fig. 6 shows the simulation result for an acceleration of the motor from 0 to 3000 rpm, corresponding to 200% the base speed, while Fig. 7 shows the corresponding diagrams of the current i_q and i_d.

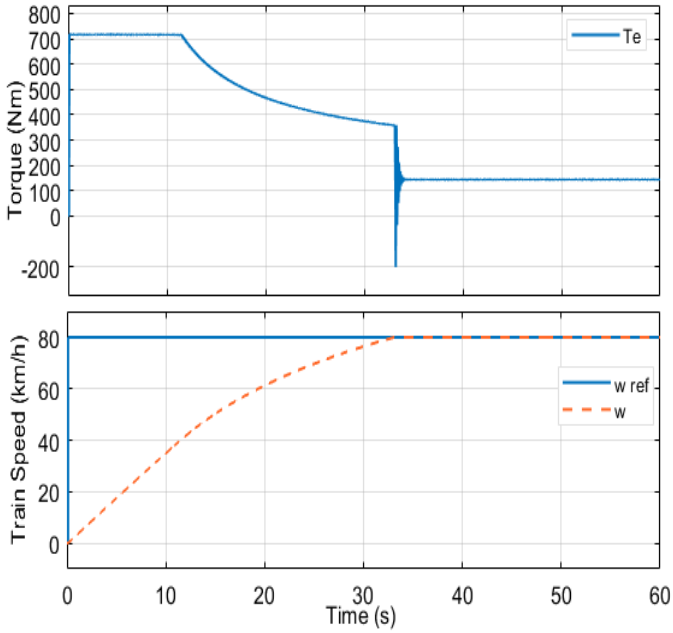

Fig. 5 Speed and Torque reference of SMPMSM with FW

When looking at Fig. 7, it can be clearly seen that the above the base speed the current id must be substantially increased to enable FW and, at the speed of 3000 rpm, the angle γ is equal to 82.2°.

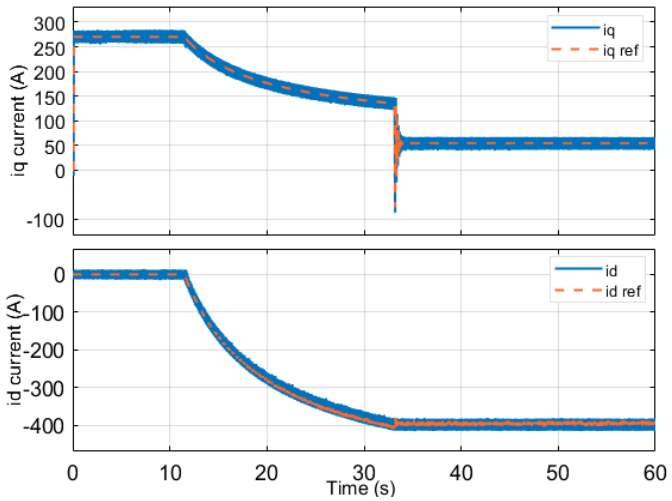

Fig. 6 Currents i_q and i_d and their reference for SMPMSM with FW

The IPMSM model is shown in Fig. 8 and uses MTPA, and FW as shown in section IV.

The saliency ratio has key role to determine the torque capabilities and speed range. There exist some studies to estimate and calculate the saliency ratio. For instance, [21] uses injection technique and claims that the saliency ratio is $L_q=(2/3)L_d$ for IPMSM in practice. Lumped parameter magnetic circuit model (LPMSM) [22], winding function theory (WFT) with LPMSM [23]and finite element method (FEM) [24] are proposed to find L_d and L_q values for IPMSM. Also, [25] compares large, low, and inverse saliency effects on the IPMSM. According to [26], saliency ratio is around between 2 and 3 for traditional IPMSM. These L_d and L_q parameters cannot be derived exactly without having the machine for inductance measurements. Therefore, based on the given parameters in datasheet 50% of magnetising inductance is added to L_d and subtracted from L_q in order to meet the criteria given in [26]. Finally, the L_d and L_q inductances for the IPMSM motor are yielded as 1.5525 mH and 0.6555 mH respectively. A simulation for this model has been carried out for the same conditions of SMPMSM, i.e., an acceleration from standstill up to a speed of 3000 rpm. Fig. 9 shows the speed and torque diagrams, while Fig. 10 shows the diagrams of the currents i_d and i_q.

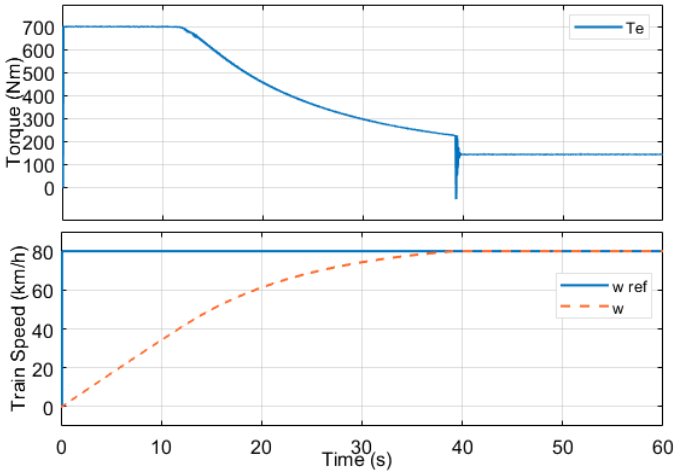

Fig. 7 Speed and torque reference of IPMSM with FW

The figures show that up to the base speed the IPMSM produces slightly less torque than SMPMSM type with less current due to flux linkage of magnetic material. In terms of demagnetisation of magnet, same amount of torque with less current is desired to protect magnetic feature of magnets. Therefore, almost the same torque with less current must be traded off against the additional complexity in the design of IPMSM and the additional weight and cost of magnets to keep the same flux linkage. Nevertheless, due to the required high

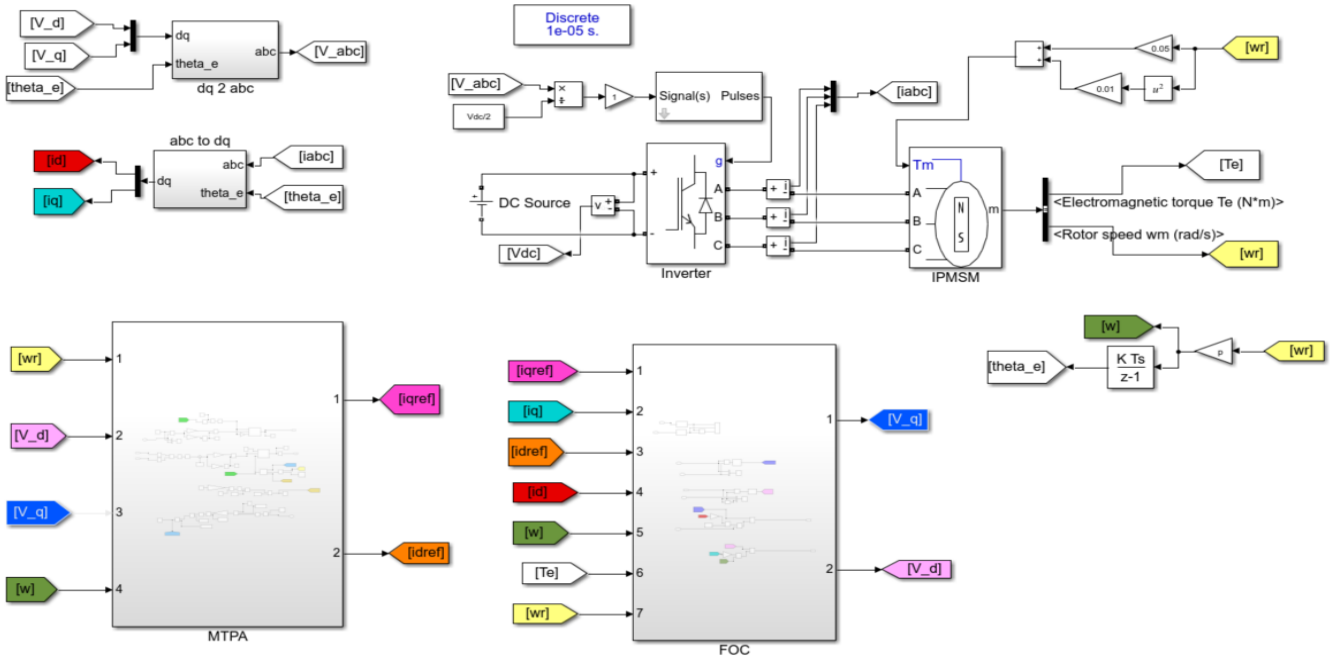

Fig. 8 Simulink Model of IPMSM with MTPA

speed of the motor, this is partially compensated by the need of robust bandages on SMPMSM to keep the mechanical integrity of the rotor. Conversely, if the same base torque is required, IPMSM can operate with smaller current and then have a higher efficiency, or can be designed with smaller coils reducing weight, volume, and cost.

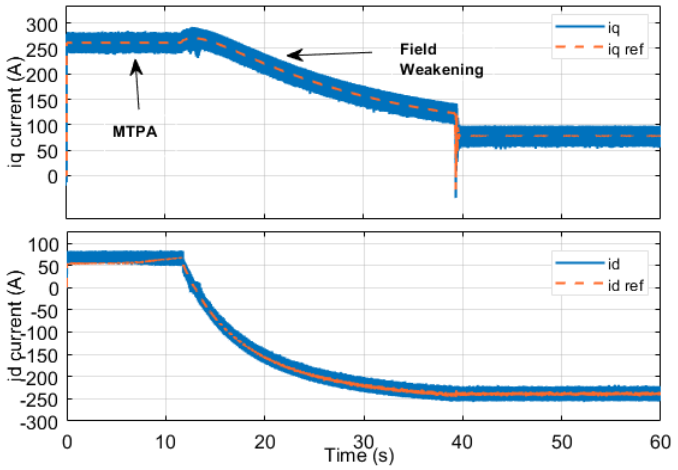

Fig. 8 Currents i_d and i_q their references for IPMSM

The angle increases from 0 degrees up to the base speed to 72.1 degrees at 3000 rpm. It can be clearly seen that the demagnetising current i_d of IPMSM is much lower than SMPMSM, which is a benefit in terms of risk of demagnetisation.

VI. Conclusion

This study investigated MTPA and FW strategies for both SMPMSM and IPMSM which used in light railway applications.

Simulation results showed that IPMSM operates less current than SMPMSM with the same output torque, albeit with more magnets maintain the same flux linkage. If instead the same current is dragged, IPMSM can produce more torque compared to SMPMSM and the motor is more efficient.

In FW operations, IPMSM achieve the same speed with a lower demagnetising current than SMPMSM and hence are preferred for traction applications where the maximum speed is typically 2-3 times the base speed.

References

[1] M. Brenna, F. Foiadelli, D. Zaninelli, Electrical Railway Transportation Systems, New Jersey: IEEE Press Wiley, 2018.

[2] S. Hillmansen, F. Schmid, T. Schmid, "The Rise of The Permanent-Magnet Traction Motor," *Railway Gazette International*, pp. 30-34, February 2011.

[3] S. Kim, Electric Motor Control, Oxford: Elsevier Inc., 2017.

[4] C. C. Chan, Chunhua Liu, K. T. Chau, "Overview of Permanent-Magnet Brushless Drives for Electric and Hybrid Electric Vehicles," *IEEE Trans. Ind. Electron.*, vol. 55, no. 6, p. 2246–2257, Jun. 2008.

[5] Ş. Kuşdoğan, "Elektrikli Otomobillerde Enerji Depolama Sistemlerindeki Gelişmeler," *Mühendis ve Makine*, vol. 50, no. 596, pp. 2-11, 2009.

[6] D. Bidart, M. Pietrzak-David, P.l Maussion, and M. Fadel, "Mono Inverter Multi-Parallel Permanent Magnet Synchronous Motor: Structure and Control Strategy," *IET Electric Power Applications*, vol. 5, no. 3, pp. 288-294, 2011.

[7] T. Nagano, J. Itoh, "Parallel Connected Multiple Drive System Using Small Auxiliary Inverter for Numbers of PMSM," in *International Power Electronics Conference (IPEC-Hiroshima 2014 - ECCE ASIA)*, 2014.

[8] A. Bouscayrol, M. Pietrzak-David, P. Delarue, R. Pefta-Eguiluz, P. V. Kestelyn, "Weighted Control of Traction Drives With Parallel-Connected AC Machines," *IEEE Trans. Industrial Electronics*, vol. 53, no. 6, pp. 1799-1806, 2006.

[9] M. Galea, *Advanced AC Drives. Lecture Notes, Topic: "Torque production in Salient PMSM"*, Nottingham: Department of Electrical and Electronic Engineering, University of Nottingham, 2017.

[10] S. Lim, "Sensorless-FOC With Flux-Weakening and MTPA for IPMSM Motor Drives," Texas Instruments Incorporated, Dallas, Texas, April 2018.

[11] S. Wang, M. Chen, M. Jiang, H. Yuan, H. Yu, J. Li, "Research on Speed Expansion Capability of Hybrid Permanent Magnet Synchronous Motor," in *IEEE 3rd Conference on Energy Internet and Energy System Integration (EI2)*, Changsha, China, 2019.

[12] Y. Li, S. Zhao, Y. Zhao, "Stduy on Flux Weakening Speed Regulation of Permanent Magnet Synchronous Motor for Vehicle," in *Chinese Control And Decision Conference (CCDC)*, 2019.

[13] C. Capitan, *Torque Control in Field Weakening Mode*, Aalborg: Aalborg University, 2009.

[14] M. Li, *Flux-Weakening Control for Permanent-Magnet Synchronous Motors Based on Z-Source Inverters*, Milwaukee, Wisconsin: e-Publications@Marquette, 2014.

[15] H. Gashtil, V. Pickert, D. Atkinson, D. Giaouris, and M. Dahidah, "Comparative Evaluation of Field Oriented Control and Direct Torque Control Methodologies in Field Weakening Regions for Interior Permanent Magnet Machines," in *2019 IEEE 13th International Conference on Compatibility, Power Electronics and Power Engineering (CPE-POWERENG)*, 2019.

[16] J. Winnett, A. Hoffrichter, A. Iraklis, A. McGordon, D. J. Hughes, T. Ridler, N. Mallinson, "Development of A Very Light Rail Vehicle," *Proceedings of the Institution of Civil Engineers: Transport*, vol. 170, no. 4, pp. 231-242, 2017.

[17] C. Beech, *Gearing*, The Technical Committee Illustrations, 1993.

[18] I. Alcalá, A. Claudio, G. Guerrero, J. A. Alquicira, V. H. Olivares, "Electric Vehicle Emulation Based On Inertial Flywheel and A DC Machine," *Dyna*, vol. 81, no. 183, pp. 86-96, 2014.

[19] P. Fajri, R. Ahmadi, M. Ferdowsi, "Equivalent Vehicle Rotational Inertia Used for Electric Vehicle Test Bench Dynamic Studies," in *IECON Proceedings (Industrial Electronics Conference)*, 2012.

[20] S. Vaez-Zadeh, Control of Permanent Magnet Synchronous Motors, Oxford: Oxford University Press, 2018.

[21] P. Brandstetter, T. Krecek, "Estimation of PMSM Magnetic Saliency Using Injection Technique," *Elektronika Ir Elektrotrchnika*, vol. 20, no. 2, pp. 22-27, 2014.

[22] K. Lee, J. Lee, H. Lee, "Inductance Calculation of Flux Concentrating Permanent Magnet Motor through Nonlinear Magnetic Equivalent Circuit," *IEEE Transactions on Magnetics*, vol. 51, no. 11, 2015.

[23] P. Liang, Y. Pei, F. Chai, and K. Zhao, "Analytical Calculation of D- and Q-axis Inductance for Interior Permanent Magnet Motors Based on Winding Function Theory," *Energies*, vol. 9, no. 580, 2016.

[24] Q. Li, J. Shang, "Experimental Measurement and FEM Calculations of the Inductance Parameters in SRM," in *2010 First International Conference on Pervasive Computing, Signal Processing and Applications*, 1273–1276, 2010.

[25] W. Wu, X. Zhu, L. Quan, Y. Hua, and Q. Lu, "Comparative Study of IPM Synchronous Machines with Different Saliency Ratios Considering EVs Operating Conditions," *Progress In Electromagnetics Research*, vol. 71, pp. 19-29, 2018.

[26] R. Krishnan, Electric Motor Drives: Modeling, Analysis, and Control, Prentice Hall, 2001.